IOSR Journal of Applied Chemistry (IOSR-JAC)
e-ISSN: 2278-5736.Volume 13, Issue 2 Ser. I (February. 2020), PP 65-72
www.iosrjournals.org

Energy and Electron Transfer in Unsymmetrical Bimetallic Complexes: Experimental and Theoretical Investigations

[1]Aaron I. Baba, *[2]Simeon Atiga, [2]Adejoh Ocheni
[1](Department of Chemistry, Federal University Lokoja, P.M.B.1154, Lokoja, Kogi State, Nigeria)
[2](Department of Chemistry, Kogi State University, P.M.B 1008, Anyigba, Kogi State, Nigeria)

Abstract: *Various unsymmetrical bimetallic complexes of ruthenium and rhenium with the ligand, 1,4-bis(4'-methyl-2,2'-bipyrid-4-yl)benzene**(bphb)**, incorporatingCH_3CN, pyridine (py),bipyridine (bpy), N-methyl-imidazole (NMI), terpyridine (terpy) and 4,4'-diethyl-carboxy-2,2'-bipyridine (decb) were synthesised and characterised by fast atomic bombardment mass spectroscopy. Electrochemical studies reveal two oxidative peaks equivalent to two metal centres. Although the reductive electrochemistry consisted of several overlapping peaks, some of the peak potentials were discerned. In most cases, the complexes showed absorption peaks at 460 (+/-10) nm with a shoulder at 350nm for Re(I) containing complexes, and additional peaks at 480nm for tpy and CN complexes. Emission from the acceptor moieties were identified at room temperature and at 77K. Electron transfer is endergonic (ΔG>0) in the complexes, and the calculated energy transfer rate constants are much smaller than the experimental values. Energy transfer was observed to be dominated by Dexter (exchange) mechanism, with little Forster mechanism contribution.*

Date of Submission: 18-02-2020 Date of Acceptance: 02-03-2020

I. Introduction

Intramolecular energy and electron transfer are very important in natural processes such as photosynthesis and respiration.[1,2] Synthesis of artificial photosystems akin to natural systems, with potential utility as photochemical devices is based on the design strategy of both donor and acceptor centres linked via molecular bridge(s).[3] Investigation of such systems provide information about the mechanism of transfer between the donor and acceptor ends[4], the effect of nature of the bridging ligand and their relations to fundamental electron and/or energy transfer theories,[5,6] and their potential application as molecular devices.[7,8]

Over the years, several investigators have studied photoinduced electron and/or energy transfer reactions in donor and acceptor systems,[9,10,11,12,13] most of which involved long synthetic schemes, low photochemical yields and/or photochemical processes that are complicated by conformational changes.

In this report, we describe an investigation of photoinduced electron and/or energy transfer in donor-acceptor systems that are bridged by ligands with defined geometry and that also provide good electronic communication between both centres.

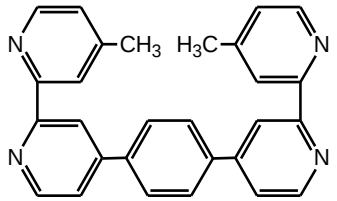

bphb

The ligand, **bphb**(1,4-bis(4'-methyl-2,2'-bipyrid-4-yl)benzene), has a well-defined geometry and the symmetric bimetallic complex, $[(dmb)_2Ru(bphb)Ru(dmb)_2](PF_6)_2$, where **dmb** is 4,4'-dimethyl-2,2'-bipyridine, has a very long room temperature lifetime and high quantum yield. Based on these properties which are desirable in the design of artificial photosystems, the **bphb** ligand was used to prepare unsymmetrical donor-acceptor complexes. The donor and acceptor moieties were selected with the intention of varying the energy gap in the resulting complexes. The spectroscopic properties of these complexes were investigated, along with the transfer mechanism in effect, in addition to the correlation between the transfer rates and the energy gaps. These transfer rates were compared with theoretical values and related to results from previous studies.[14]

II. Materials and Methods

Materials

The solvents for synthesis were used as received without additional purification. All solvents used for spectrophotometric measurements were of spectral quality. $[(bpy)_2RuCl_2]2H_2O$ and $[(tpy)RuCl_3]$ were prepared using literature methods.[15]

Measurements

Values of redox potential were obtained by cyclic voltammetry on EG and G Princeton Applied Research (PAR) model 173 Potentiostat, and differential pulse polarography, FAB-Mass spectrometry were acquired on Kratos Analytical (Manchester England) Concept 1-H mass spectrometer, while luminescence and luminescence lifetime measurements were recorded using a SpexFluorolog equipped with a 450 W Xenon arc lamp and a cooled photomultiplier tube.

Synthesis of Complexes

The ligand,**bphb** was synthesized using previous published methods. All reactions were done under nitrogen blanket and all metal complexes prepared were finally dissolved in a small volume of acetone or acetone reprecipitated from diethyl ether.

$[(bpy)_2Ru(bphb)](PF_6)_2$was prepared from $[(bpy)_2RuCl_2]2H_2O$ (220 mg, 0.423 mmoles) and bphb ligand (1.3 g, 3.38 mmoles). The bphb ligand was refluxed for 1 hr in a mixture of 80 ml $CHCl_3$ and 100 ml EtOH, after which the $(bpy)_2RuCl_2.2H_2O$ which was dissolved in 20 ml of EtOH was added dropwise from a dropping funnel. The mixture was refluxed for additional 2 hrs and then rotary evaporated to dryness, dissolved in H_2O and filtered. The residue was washed thoroughly with more H_2O and the product precipitated from the filtrate by dropwise addition of saturated solution of NH_4PF_6. The precipitate was collected and dried. The presence of one single product was confirmed by a single spot on a neutral alumina TLC plate using toluene:acetonitrile (2:1) as eluent. Yield: 430 mg (90%), FAB-MS: 1099.07 (M); 945.1 (M-PF_6); 809 (M-$2PF_6$).

$\{[(bpy)_2Ru]_2bphb](PF_6)_4$ was prepared by refluxing $[(bpy)_2RuCl_2]2H_2O$ (232 mg, 0.447 mmoles) and **bphb** (69mg, 0.179 mmoles) in 50 ml EtOH for 3 hrs. The mixture was rotary evaporated to dryness and the residue dissolved in water. After filtration, the product was precipitated from the filtrate by dropwise addition of a saturated solution of NH_4PF_6 and the product collected and dried. The product was purified by chromatography on acidic alumina column using toluene:acetronitrile (1:1) as eluent. Yield: 250 mg (78%) FAB-MS: 1794.01(M); 1648.6 (M-PF_6); 1504.6 (M-$2PF_6$).

$[(bpy)_2Ru(bphb)Re(CO)_3(Cl)](PF_6)_2$. This compound was prepared using modification to an earlier published method.[16]$Re(CO)_5Cl$ (117 mg, 0.322 mmoles) was sonicated to dissolve in 40 ml of methanol and was added to 80 ml solution of $[(bpy)_2Ru(bphb)](PF_6)_2$ (300 mg, 0.275 mmoles). The mixture was refluxed for 9 hrs, cooled and rotary evaporated to 40 ml before saturated solution of NH_4PF_6 in methanol was added dropwise to precipitate the product. The product was collected by suction filtration, washed with diethyl ether and air dried. Yield; 280 mg (70%).

$[(bpy)_2Ru(bphb)Re(CO)_3(CH_3CN)](PF_6)_3$: $[(bpy)_2Ru(bphb)Re(CO)_3(Cl)](PF_6)_2$. (240 mg, 0.172 mmoles) was refluxed for 7 hrs with $AgPF_6$ (217 mg, 0.86 mmoles) in 40 ml CH_3CN. The solution was cooled, rotary evaporated to 5 ml and chromatographed on acidic alumina using CH_3CN as eluent, to remove any $[(bpy)_2Ru(bphb](PF_6)_2$ impurity and AgCl. Yield: 200 mg (75%). IR (c=o stretch) = 2038, 2021, 1921. FAB-MS: 1547.05 (M); 1402.2 (M-PF_6); 1256.3 (M-$2PF_6$);

$[(bpy)_2Ru(bphb)Re(CO)_3(NMI)](PF_6)_3$: $[(bpy)_2Ru(bphb)Re(CO)_3(CH_3CN)](PF_6)_3$ (80 mg, 0.0573 mmoles) was refluxed for 2 hrs in 20 ml THF along with N-methyl imidazole (1.5 ml, 0.019 mmoles). The mixture was rotary evaporated to dryness and purified on glass beads using CH_3CN as eluent and again rotary evaporated to dryness. Yield: 50 mg (55%). IR (c=O stretch) = 2029, 1925, 1913. FAB-MS: 1588.08 (M); 1444.3 (M-PF_6); 1298.4 (M-$2PF_6$).

$[(bpy)_2Ru(bphb)Re(CO)_3(Py)](PF_6)_3$ was prepared from $[(bpy)_2Ru(bphb)Re(CO)_3(CH_3CN)](PF_6)_3$. (80 mg, 0.0573 mmoles) and pyridine (1 ml) using the same procedure as for $[(bpy)_2Ru(bphb)Re(CO)_3(NMI)](PF_6)_3$. Yield: 55 mg (60%). FAB-MS: 1585.07 (M); 11235.5 (M-PF_6); 1090.5 (M-$2PF_6$); 945.5 (M-$3PF_6$).

$[(bpy)_2Ru(bphb)Ru(tpy)(CN)](PF_6)_3$ $[(bpy)_2RuCl_2]2H_2O$ (50mg, 0.046mmoles) and $[(tpy)RuCl_3]$ (30.36 mg, 0.046 mmoles) were refluxed in 25 ml ethanol/water (3:1, v/v) for 4 hr under an argon blanket. 0.5 g of KCN which was dissolved in 5 ml H_2O was added and the solution refluxed for additional 2 hr. The solution was cooled and rotary evaporated to half the original volume. The crude product formed was precipitated by addition of a saturated solution of NH_4PF_6. The precipitate was filtered, rinsed with 5 ml H_2O and was air dried before being chromatographed on a glass bead column using CH_3CN/toluene (1:1) as eluent. The first red band

was collected and rotary evaporated to dryness. Yield: 46 mg (68.9%). FAB-MS: M-PF_6=1451.1 (1450.1), M-$2PF_6$=1306.1 (1305.22).

$[(decb)_2Ru(bphb)Re(CO)_3(CH_3CN)](PF_6)_3$ $(decb)_2RuCl_2$ (157 mg, 0.20 mmoles) and $AgNO_3$ (169 mg, 0.94 mmoles) were refluxed in 40 ml MeOH for 8 hrs. This mixture was transferred via cannula to a refluxing solution of $[Re(CO)_3(bphb)Cl]$ (280 mg, 0.405 mmoles) and tetraethyl ammonium chloride (70 mg, 4.22 mmoles) in 80 ml MeOH. The combined mixture was refluxed for additional 15 hrs, cooled, filtered and rotary evaporated to near dryness. The residue was dissolved in water and filtered again before a saturated solution of NH_4PF_6 was added dropwise. The product, $[(decb)_2Ru(bphb)Re(CO)_3(Cl)](PF_6)_2$ was collected and dried. Yield: 210 mg. The $[(decb)_2Ru(bphb)Re(CO)_3(Cl)](PF_6)_2$ was refluxed with $AgPF_6$ (180 mg, 7.12 mmoles) in 40 ml CH_3CN for 7 hrs, cooled and rotary evaporated to dryness. The residue was purified by chromatography on neutral alumina column using toluene:acetonitrile (2:1) as eluent. The first fraction consisted of a mixture of unreacted rhenium monomer and $(decb)_2RuCl_2$ while the later fraction consisted of the product. Yield: 90 mg. FAB-MS were very weak.

$[(tpy(CN)Ru(bphb)Re(CO)_3(CH_3CN)](PF_6)_3$ $[Ru(tpy)(CN)(bphb)](PF_6)$ (80 mg, 0.0898 mmoles) in 35 ml MeOH and $[Re(CO)_5Cl$ (38 mg, 0.105 mmoles) in 20 ml MeOH were reacted as described for $[(bpy)_2Ru(bphb)Re(CO_3)Cl](PF_6)_2$ to yield 100 mg (83%) of $[(tpy(CN)Ru(bphb)Re(CO)_3(Cl)](PF_6)$. The $[(tpy(CN)Ru(bphb)Re(CO)_3(Cl)](PF_6)$ was refluxed with 100 mg (3.95 mmoles) $AgPF_6$ in 40 ml CH_3CN for 4 hrs, cooled and rotary evaporated to dryness. The residue was purified first by chromatography on acidic alumina column using CH_3CN as eluent, to remove unreacted $[Ru(tpy)(CN)(bphb)](PF_6)$, and later on glass beads using CH_3CN to remove decomposed product. After rotary evaporation, 50 mg of pure product was obtained. FAB-MS peaks were very weak.

$[(tpy(CN)Ru(bphb)Ru(tpy)(CN)](PF_6)_2$ $[(tpy)RuCl_3$ (186 mg, 0.423 mmoles) was refluxed in 20 ml of ethanol/water (50:50, v/v) for 30 mins under an argon blanket until it dissolved, then 90 mg (0.23 mmoles) of **bphb** was added. The solution was refluxed for 4 hrs and 0.5 g of KCN which was dissolved in 5 ml H_2O was added. The solution was refluxed for another 1 hr before half of the solution was rotary evaporated. The crude product was precipitated by addition of saturated solution of NH_4PF_6 and later air dried. The collected product was washed with diethyl ether to remove unreacted **bphb** ligand, followed by washing with water. The solid was chromatographed on acidic alumina first using CH_3CN eluent. Second purification involved the use of CH_3CN/ethanol (50:50, v/v as eluent. The deep red band with maximum absorbance at 496 nm was collected and rotary evaporated to dryness. Yield: 167 mg, 28.3%. FAB-MS: M-PF_6= 1253.3 (1252.1), M-$2PF_6$ = 1107.2 (1107.1).

III. Results And Discussion

Syntheses

The $[(bpy)_2Ru(bphb)](PF_6)_2$ based unsymmetrical bimetallic complexes were synthesized via the monomers to prevent contamination from free non-linked donor impurities. For example, the synthesis of $[(bpy)_2Ru(bphb)Re(CO)_3(L)](PF_6)_3$ began with the complexation of $[(bpy)_2Ru(bphb)](PF_6)_2$ with $[Re(CO)_3Cl]$ to form $[(bpy)_2Ru(bphb)Re(CO)_3(Cl)](PF_6)_3$. The chloride ligand was then substituted with CH_3CN, from which the N-methyl-imidazole and pyridine derivatives were made. An exception to this synthetic approach was $[(decb)_2Ru(bphb)Re(CO)_3(CH_3CN)](PF_6)_3$ which was prepared differently because of the ease of hydrolysis of the **decb** ligand. This series of complexes were all bridged by the **bphb** ligand.

Electrochemistry

The redox properties of the complexes are given in Table 1. The unsymmetrical bimetallic complexes all have two oxidative peaks corresponding to the two metal centres. For most of the complexes, especially the **Ru-Re** systems, the second oxidative peak is usually lower in peak height and area, and it is assigned to the acceptor. For instance, the oxidation sequence of $[(bpy)_2Ru(bphb)Re(CO)_3(CH_3CN)]_{3+}$ is given in eq. 1 and 2.

Table 1: Redox Potentials of Donor-Acceptor Complexes examined in CH_3CN

	Oxidation		Reduction	
Compound	E_1, V	E_2, V	$-E_3$, V	$-E_4$,V
$[(bpy)_2Ru(bphb)Re(CO)_3(CH_3CN)]^{3+}$		1.80	1.30	1.021.23
$[(bpy)_2Ru(bphb)Re(CO)_3(NMI)]^{3+}$	1.61	1.27	1.081.28	
$[(bpy)_2Ru(bphb)Re(CO)_3(Py)]^{3+}$	1.79	1.29	1.021.07	
$[(decb)_2Ru(bphb)Re(CO)_3(CH_3CN)]^{3+}$	1.79	1.45	0.921.10	
$[(tpy)(CN)_2Ru(bphb)Re(CO)_3(CH_3CN)]^{2+}$	1.791.25		1.32	
$[(bpy)_2Ru(bphb)Ru(tpy)(CN)]^{3+}$	1.32	1.11	1.221.36	
$\{[(bpy)_2Ru]_2bphb]^{4+}$		1.24		1.241.32
$[(decb)_2Ru(bphb)^{2+}$		1.40		0.951.09

All potentials are in volts and were recorded by cyclic voltammetry (100mV/sec) and differential pulse polarography (5mV/sec, pulse height=20mV) in CH_3CN containing 0.1 M tetraethylammonium perchlorate.

$[(bpy)_2Ru(II)(bphb)Re(I)(CO)_3(CH_3CN)]^{3+} \leftrightarrow [(bpy)_2Ru(III)(bphb)Re(I)(CO)_3(CH_3CN)]^{4+}$ (1)

$[(bpy)_2Ru(III)(bphb)Re(I)(CO)_3(CH_3CN)]^{4+} \leftrightarrow [(bpy)_2Ru(III)(bphb)Re(II)(CO)_3(CH_3CN)]^{5+}$ (2)

The oxidation potentials obtained are comparable to those of mononuclear or symmetrical bimetallic complexes[17]**.** The reductive electrochemistry consists of several overlapping peaks, but it is still possible to discern some of the peak potentials. As with the Ru(II) and Re(I) dimer complexes, the first reduction is localized on the ligand with the lowest unoccupied molecular orbital. The second reduction, which is assigned to the Re(II/I) couple, overlaps with several reductions of ligands on the other metal.

Absorption and Luminescence Properties

The absorption and the luminescence data are provided in Table 2. These complexes showed a single absorption peak. Most of them have absorption maxima at 460nm (+/-10 nm). A closer look at the absorption spectra of the Re(I) containing complexes reveal a shoulder around 350 nm, which might be due to the Re(I) Metal-to-Ligand-Charge-Transfer (MLCT) transition. Also the **tpy** and **CN** containing complexes show additional absorption peaks beyond 480 nm.

Emission spectra obtained at both room temperature and 77K for the unsymmetrical bimetallic complexes are dominated by emission from the acceptor moiety. The donor end emission was not observed, except for $[(tpy)(CN)_2Ru(bphb)Re(CO)_3(CH_3CN)]^{2+}$ which shows a small shoulder to the blue end of the dimer emission at 77K. This observation may reflect strong emission quantum yield for the acceptor moiety or fast electronic energy transfer to the acceptor centre. The emission quantum yield of the bimetallic complex donor is decreased by energy transfer. If $K_{en}>>K_r$, then emission quantum yield becomes too small to measure.

The emission lifetime for donor luminescence in these complexes was very short both at room temperature and at 77K but could be measured for $[(tpy)(CN)_2Ru(bphb)Re(CO)_3(CH_3CN)]^{2+}$and $[(bpy)_2Ru(bphb)Ru(tpy)(CN)]^{3+}$. The respective lifetimes are 0.09 ns (+/-0.002 ns) and 6.1 ns (+/-0.02 ns). For the other members of the series, the lifetime was too short to measure even with the picosecond time-correlated single photon counting equipment. On the contrary, the symmetrical bimetallic complexes have long and biexponential lifetimes as have been reported for other Re(I) complexes.[18, 19] This implies that, for the unsymmetrical bimetallic complexes, energy transfer between the donor and acceptor centres is fast.

Table 2: Spectroscopic Properties of Metal Complexes examined

Compound	λ_{abs}	logε	λem (RT)	λem (77k)	τ_{em}(RT)
$[(bpy)_2Ru(bphb)Re(CO)_3(CH_3CN)]^{3+}$	456	4.56	619	517, 541, 586-	
$[(bpy)_2Ru(bphb)Re(CO)_3(NMI)]^{3+}$	456	4.20	628	598, 645-	
$[(bpy)_2Ru(bphb)Re(CO)_3(Py)]^{3+}$	458	4.23	614	586, 630, 700-	
$[(decb)_2Ru(bphb)Re(CO)_3(CH_3CN)]^{3+}$	466	4.51	638	608, 654-	
$[(tpy)(CN)_2Ru(bphb)Re(CO)_3(CH_3CN)]^{2+}$	468	4.2	545,600	638, 5960.09	
$[(bpy)_2Ru(bphb)Ru(tpy)(CN)]^{3+}$	464	4.54	656	640	6.10
$\{[(bpy)_2Ru]_2bphb]^{4+}$	462	4.61	626	598, 6451950	
$[(decb)_2Ru(bphb)^{2+}$	468	4.70	644	612, 6621450	

Samples were degassed in CH_3CN for 5 mins.Emission lifetimes refer to luminescence from the donor end

In principle, there is a possibility of oxidative and reductive electron transfer quenching of the donor. To illustrate with the complex $[(bpy)_2Ru(bphb)Re(CO)_3(CH_3CN)]^{3+}$, after photoexcitation (eq. 3), the donor can undergo reductive (eq. 4) or oxidative quenching (eq. 5).

$[(bpy)_2Ru(II)(bphb)Re(I)(CO)_3(CH_3CN)]^{3+} \leftrightarrow [(bpy)_2Ru(II)(bphb)Re^*(I)(CO)_3(CH_3CN)]^{3+}$ (3)

$[(bpy)_2Ru(II)(bphb)Re^*(I)(CO)_3(CH_3CN)]^{3+} \leftrightarrow [(bpy)_2Ru(III)(bphb)Re(I)(CO)_3(CH_3CN)]^{3+}$ (4)

$[(bpy)_2Ru(II)(bphb)Re^*(I)(CO)_3(CH_3CN)]^{3+} \leftrightarrow [(bpy)(bpy\text{-})Ru(II)(bphb)Re^*(II)(CO)_3(CH_3CN)]^{3+}$ (5)

The free energy of both electron transfer processes can be calculated from the emission energy and the redox potentials of the complexes using the Rehm-Weller relation (eq 6).

$\Delta G = E_{ox}(D) - E_{red}(A) - E_{oo} + C$ (6)

This relation considers the oxidation potential of the donor, $E_{ox}(D)$, the reduction potential of the acceptor, $E_{red}(A)$ and the emission energy, E_{oo}.The E_{oo} is taken as the room temperature emission energy in electron volts (V), while $E_{ox}(D)$ and $E_{red}(A)$ are the oxidation and reduction potentials of the symmetric bimetallic or monometallic donor complexes. C is the coulombic term which describes the electrostatic interaction of the centres as they are brought together. This term will be unimportant for covalently linked donor-acceptor complexes.

For the complex $[(bpy)_2Ru(II)(bphb)Re(I)(CO)_3(CH_3CN)]^{3+}$, the Ru(2+/3+) = 1.30 V, Re (+/2+) = 1.80 V, Re(+/0) = Ru(2+/+) = -1.023 V, Eoo = 2.23 V. The free energy for oxidative quenching, ΔE(0x) = -0.59 V, while the reductive quenching, ΔEel(red) = - 0.09 V. From the relationship, ΔG = -nF(ΔE), the electron transfer process will be endergonic (ΔG>0) for all the complexes in this series, based on the ΔEel(red) and ΔEel(ox values in Table 2. On the contrary, energy transfer quenching (eq. 7) is energetically favoured

$[(bpy)_2Ru(II)(bphb)Re^*(I)(CO)_3(CH_3CN)]^{3+} \leftrightarrow [(bpy)_2Ru^*(II)(bphb)Re(I)(CO)_3(CH_3CN)]^{3+}$

Energy transfer processes are indicated by rise times in the acceptor decay profiles or quenching (reduction) in the donor emission. Emission rise times are seldom observed in transition metal complexes because of strong overlap between donor and acceptor absorptions which makes selective donor excitation difficult. As a result, most energy transfer processes are marked by donor emission quenching. However, at low temperature (around 5K) the time-resolved luminescence of the donor centre of $[(dmb)_2Ru(bdebb)Ru(biq)]^{4+}$ shows a rise and fall.[20]

The energy transfer rate is obtained from the relationship:

$k_{en} = (1/\tau_{DA}) + (1/\tau_D)(s^{-1})$ (7)

where τ_{DA} and $\tau_D$are the emission lifetime of the donor-acceptor complex and donor complex, respectively.

Mechanism of Energy Transfer

Energy transfer processes in donor-acceptor complexes involve excitation of the donor centre which relaxes back to the lowest thermally-equilibrated energy excited state, followed by energy transfer from the donor to the acceptor, and finally relaxation of the donor to the ground state or to products, in competition with back energy transfer.[21] The mechanism of energy transfer between the donor and acceptor complexes can be described by two mechanisms: Forster and Dexter.

The Forster mechanism is based on the overlap of the donor emission and acceptor absorption.[22] Donor and acceptor complexes having large energy gaps between the donor and acceptor moieties will have large overlap and more contribution from the Forster mechanism.[23] The energy transfer via this mechanism is given by eq. 8, which is the same as eq. 7[24]

$$k_{en} = 1.25 \times 10^{17} \left[\frac{\varphi_{em}}{\eta^4 \tau_D R^6}\right] \int_0^\infty I_D \varepsilon_A \frac{d\bar{\nu}}{\bar{\nu}^4} \quad (8)$$

$\int_0^\infty I_D \varepsilon_A \frac{d\bar{\nu}}{\bar{\nu}^4}$ = Forster overlap, numerically calculated from donor emission and acceptor absorption overlap

The donor-acceptor distance is R=11.3A^0, based on an X-ray crystal structure of the bridging ligand, **bphb**[25].

The solvent's (acetonitrile) refractive index, η is 1.39. ϕ_{em} and $\tau_D$are the donor emission quantum yield and lifetime, respectively; their values are given in Table 3. The overlap integral is obtained from the integrated area of the normalized donor emission and acceptor absorption spectra as illustrated in Fig. 1.The calculated Forster Overlap and energy transfer rate via this mechanism are given in Table 3. The calculated energy transfer rate constants are much smaller than the experimental values. Energy transfer rates in the region predicted by the Forster mechanism would be measurable using commonly available laser facilities. These results imply that, for this series of complexes, energy transfer is dominated by Dexter (exchange) mechanism, with minor contribution from Forster mechanism[24].

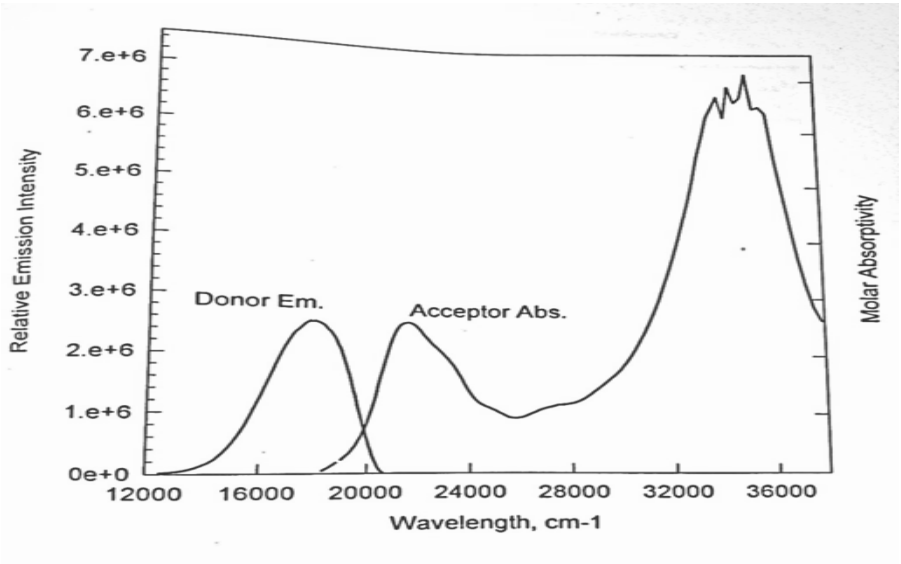

Figure. 1:A Forster overlap for the donor, $\{[Re(CO)_3AN]_2(bphb)\}(PF_6)_2$ emission and the acceptor, $\{[Ru(bpy)_2]_2(bphb)\}(PF_6)_4$ absorption. The overlap area was numerically calculated to obtain the Forster overlap

When the emission lifetimes are measurable, the contribution of Dexter (exchange) mechanism to the energy transfer process can be determined by subtracting the calculated luminescence decay rate based on eq. 8 from the experimentally measured rates.

Table 3: Parameters Used to Verify Energy Transfer by Forster Mechanism

Compound	ΔE^a	$\Delta E_{el}(ox)^b$	$\Delta E_{el}(red)^b$	FO^c	$K_r(calc), s^{-1,d}$
$[(bpy)_2Ru(bphb)Re(CO)_3(CH_3CN)]^{3+}$	2070	-0.59	-0.09	$1.39x10^{-14}$	$2.58x10^7$
$[(bpy)_2Ru(bphb)Re(CO)_3(NMI)]^{3+}$	860	-0.60	-0.26	$6.25x10^{-18}$	$4.13x10^5$
$[(bpy)_2Ru(bphb)Re(CO)_3(Py)]^{4+}$	1446	-0.65	-0.15	$1.16x10^{-14}$	$2.21x10^7$
$[(decb)_2Ru(bphb)Re(CO)_3(CH_3CN)]^{3+}$	2457	-0.48	-0.14	$4.88x10^{-14}$	$9.60x10^7$
$[(tpy)(CN)_2Ru(bphb)Re(CO)_3(CH_3CN)]^{2+}$	3079	-0.85	-0.34	$2.10x10^{-14}$	$9.60x10^7$
$[(bpy)_2Ru(bphb)Ru(tpy)(CN)]^{3+}$	1003	-0.48	-0.35	$7.25x10^{-19}$	$1.13x10^3$

[a]Energy gap, ΔE (cm^{-1}) was determined as the difference between donor and acceptor emission maxima.
[b]Free energy of electron transfer (in volts) was calculated using eq. 6.
[c]Forster Overlap was obtained from the integral of donor emission and acceptor absorption.
[d]Energy transfer rate was calculated using eq.9.

Theoretically, the Dexter (exchange) transfer can be rationalised using the Golden Rule formalism, eq. 9 and utilizing the calculated electronic coupling matrix element, H_{AB}.

$k_{en} = \kappa FCWD$ (9)

Where $k = 4(\pi^2).[(H_{AB})^2/h]\sqrt{[1/(4\pi\, k_b \lambda\, T)]}$ (10)

And $FCWD = \Sigma\Sigma \exp(-2S).(S^w/w!)(S^y/y!).\exp\{[-\lambda - \Delta E_1 + y.h\nu_D + w.h\nu_A)2]/(4\lambda.k_b.T)\}$ (11)

$\lambda = [(\nu_h)^2/16\, K_b.\, T\, .\, \ln 2]$ (12)

By substituting the values of λ=2000cm^{-1}, $h\nu_D = h\nu_A$=1200cm^{-1}, H_{AB}=48cm^{-1}, and S=1.05 (which are typical for Ru complexes and are obtained from emission spectral fitting)[26] with the energy gap between donor and acceptor centres, ΔE_1 value of 2070 cm^{-1} for $[(bpy)_2Ru(bphb)Re(CO)_3(CH_3CN)]^{3+}$ and the calculated electronic coupling matrix element, H_{AB}, the exchange energy transfer rate constant is obtained. The dependence of the energy transfer rate constant and the emission lifetime on H_{AB} is illustrated in Table 4. With an electronic

coupling matrix element, HAB = 48cm^{-1}, the expected emission lifetime for these unsymmetrical bimetallic complexes is in picoseconds, in agreement with our inability to measure the lifetime of most of these complexes. The inability to measure the emission lifetimes also made it impossible to determine the variation of the energy transfer rate constant with the energy gap between the donor and acceptor centres. The larger transfer rate constant in these **bphb** complexes may also be due to better electronic communication, more rigidity and short distance between the donor-acceptor centres[27].

Table 4: Relationship between the Electronic Coupling Matrix Element, H_{AB} and the Rate Constant and the Expected Emission Lifetime

H_{AB}, cm^{-1}	k_{en}, s^{-1}	t, s[a]
1.00	$1.31x10^{8}$	$7.64x10^{-9}$
6.00	$4.72x10^{9}$	$2.12x10^{-10}$
11.00	$1.59x10^{10}$	$6.31x10^{-11}$
16.00	$3.35x10^{10}$	$2.98x10^{-11}$
21.00	$5.78x10^{10}$	$1.73x10^{-11}$
26.00	$8.85x10^{10}$	$1.13x10^{-11}$
31.00	$1.26x10^{11}$	$7.95x10^{-12}$
36.00	$1.70x10^{11}$	$5.89x10^{-12}$
41.00	$2.20x10^{11}$	$4.54x10^{-12}$
46.00	$2.77x10^{11}$	$3.61x10^{-12}$
51.00	$3.41x10^{11}$	$2.944x10^{-12}$

[a]*Emission lifetime values were obtained from (ken)-1. Ken values were obtained via equations 10-12 utilising typical emission spectral parameters available from literature references.*

IV. Conclusion

Forster and Dexter energy transfer mechanisms are both important in energy transfer between donor-acceptor centres in unsymmetrical compounds, but for the series of complexes investigated in this work, the Dexter (exchange) mechanism appears to be dominant. Comparison of these experimental results with others in the literature show that the bridging ligand, **bphb** is a good mediator of energy transfer processes, most probably due to its shorter distance, more rigidity and/or better electronic communication. These results provide justification for further investigation of this ligand and complexes for photochemical molecular device applications.

References

[1]. Hosseinzadeh P, Lu Y. Design and fine-tuning redox potentials of metalloproteins involved in electron transfer in bioenergetics. Biochimica et Biophysica Acta (BBA)-Bioenergetics. 2016;1857(5),557-581.

[2]. Tebo AG, Quaranta A, HerreroC, PecoraroVL, AukaulooA. Intramolecular Photogeneration of aTyrosine Radical in a Designed Protein.ChemPhotoChem. 2017;1(3),89-92.

[3]. AlbinssonB, Eng MP, PetterssonK, WintersMU. Electron and energy transfer in donor–acceptor systems with conjugated molecular bridges. Physical Chemistry Chemical Physics. 2007;9(44),5847-5864.

[4]. MirkovicT, OstroumovEE, AnnaJM, van GrondelleR, ScholesGD. Light absorption and energy transfer in the antenna complexes of photosynthetic organisms. Chemical reviews. 2016;117(2),249-293.

[5]. SunL, HammarströmL, ÅkermarkB, StyringS. Towards artificial photosynthesis: ruthenium–manganese chemistry for energy production. Chemical Society Reviews. 2001;30(1),36-49.

[6]. ScandolaF, BignozziCA, BalzaniV. Chemistry and light-part 2: light and energy. Química Nova. 1997;20(4),423-432.

[7]. Wang JW, ZhongDC, Lu TB. Artificial photosynthesis: Catalytic water oxidation and CO_2 reduction by dinuclear non-noble-metal molecular catalysts. Coordination Chemistry Reviews. 2018;377,225-236.

[8]. Gao Y, Zhang L, Ding X, Sun L. Artificial photosynthesis–functional devices for light driven water splitting with photoactive anodes based on molecular catalysts. Physical Chemistry Chemical Physics. 2014;16(24),12008-12013.

[9]. Fredin LA, Persson P. Computational characterization of competing energy and electron transfer states in bimetallic donor-acceptor systems for photocatalytic conversion. The Journal of chemical physics. 2016;145(10):104310.

[10]. AlbinssonB, Mårtensson J. Long-range electron and excitation energy transfer in donor–bridge–acceptor systems. Journal of Photochemistry and Photobiology C: Photochemistry Reviews. 2008;9(3),138-155.

[11]. PetterssonK, Kyrychenko A, Rönnow E, Ljungdahl T, Mårtensson J, Albinsson B. Singlet Energy Transfer in Porphyrin-Based Donor-Bridge-Acceptor Systems: Interaction between Bridge Length and Bridge Energy. The Journal of Physical Chemistry A. 2006;110(1),310-318.

[12]. Caprasecca S, Mennucci B.Excitation Energy Transfer in Donor-Bridge-Acceptor Systems: A Combined Quantum-Mechanical/Classical Analysis of the Role of the Bridge and the Solvent. The Journal of Physical Chemistry A. 2014;118(33),6484-6491.

[13]. HurenkampJH, de Jong JJ, Browne WR, van Esch JH, Feringa BL. Tuning energy transfer in switchable donor–acceptor systems. Organic & biomolecular chemistry. 2008;6(7),1268-1277.

[14]. LiangYY, Baba AI, Kim WY, AthertonSJ, Schmehl RH. Intramolecular exchange energy transfer in a bridged bimetallic transition metal complex: calculation of rate constants using emission spectral fitting parameters. The Journal of Physical Chemistry. 1996;100(47),18408-18414.

[15]. AdcockPA, KeeneFR, SmytheRS, SnowMR. Oxidation of isopropylamine and related amines coordinated to ruthenium. Formation of monodentate imine and alkylideneamido complexes of ruthenium. Inorganic Chemistry. 1984;23(15),2336-2343.
[16]. SahaiR, Rillema DP, ShaverR, Van Wallendael S, Jackman DC, BoldajiM. Complexes of ruthenium (II) with (2,2'-bipyrimidine) tricarbonylchlororhenium and {benzo [1,2-6:3,4-b':5,6-b"] tripyrazine} hexacarbonyldichloridirhenium as ligands: syntheses and redox and luminescence properties. Inorganic Chemistry. 1989);28(6),1022-1028.
[17]. (a)Furue M, NaikaM, KanematsuYY, KushidaT, KamachiM. Intramolecular Energy Transfer in Covalently Linked Polypyridine Rhenium(I)/Ruthenium(I1) Complexes. Cord. Chem. Rev. 1991;111,221. (b) Rilema DP, Wallendael SV. Photoinduced intramolecular energy transfer from one metal centre to the other in a mixed-metal ruthenium/rhenium complex. Cord. Chem. Rev.1991; 111, 297.
[18]. ShawJR, SchmehlRH. Photophysical properties of rhenium (I) diimine complexes: observation of room-temperature intraligand phosphorescence. Journal of the American Chemical Society. 1991;113(2),389-394.
[19]. ZippAP, Sacksteder L, StreichJ, CookA, DemasJN, DeGraffBA. Luminescence of rhenium (I) complexes with highly sterically hindered alpha-diimine ligands. Inorganic Chemistry. 1993;32(24),5629-5632.
[20]. SchmehlRH, AuerbachRA, WacholtzWF. Intramolecular energy transfer in the covalently linked dimeric complex $[(bpy)_2Ru(bb)Ru(biq)_2]^{4+.}$ The Journal of Physical Chemistry. 1988;92(22),6202-6206.
[21]. LeiY, Buranda T, EndicottJF. Photoinduced energy transfer in multinuclear transition-metal complexes. Reversible and irreversible energy flow between charge-transfer and ligand field excited states of cyanide-bridged ruthenium (II)-chromium (III) and ruthenium (II)-rhodium (III) complexes. Journal of the American Chemical Society. 1990;112(24),8820-8833.
[22]. SekarRB, PeriasamyA. Fluorescence resonance energy transfer (FRET) microscopy imaging of live cell protein localizations. The Journal of cell biology. 2003;160(5),629-633.
[23]. RowlandCE, Delehanty JB, DwyerCL, MedintzIL. Growing applications for bioassembledFörster resonance energy transfer cascades. Materials Today. 2017;20(3),131-141.
[24]. BarlthropJA, CoyleHD. Principles of Photochemistry. John Wiley and Sons, U.K.1975; Chapter 4.
[25]. WangW, BabaAI, Schmehl RH, Mague JT. A Rigid Bis-Bidentate Bridging Ligand:1,4-Bis(2,2'-bipyrid-4-yl) benzene. Acta. Cryst. 1996;C52,658-660.
[26]. BelserP, von ZelewskyA, FrankM, SeelC, VogtleF, De LuisaL, BarigelletiF, BalzaniV. Supramolecular ruthenium and/or osmium complexes of tris(bipyridine) bridging ligands. Syntheses, absorption spectra, luminescence properties, electrochemical behavior, intercomponent energy, and electron transfer. J. Am. Chem. Soc. 1993;115,4076.
[27]. ClossGL, MillerJR. Intramolecular Long-Distance Electron Transfer in Organic Molecules. Science. 1988;240,440.

2Simeon Atiga. "Energy and Electron Transfer in Unsymmetrical Bimetallic Complexes: Experimental and Theoretical Investigations." *IOSR Journal of Applied Chemistry (IOSR-JAC)*, 13(2), (2020): pp 65-72.